

Received February 2, 2021, accepted February 26, 2021, date of publication March 4, 2021, date of current version March 17, 2021.

Digital Object Identifier 10.1109/ACCESS.2021.3063768

Local Structural Optimization Method Based on Orthogonal Analysis for a Resistant Muffler

RUI LI^{1,2}, YIQI ZHOU^{1,2}, YUAN XUE³, AND SU HAN^{1,2}

¹Key Laboratory of High-Efficiency and Clean Mechanical Manufacture, Ministry of Education, Shandong University, Jinan 250061, China

²School of Mechanical Engineering, Shandong University, Jinan 250061, China

³CRRC Qingdao Sifang Corporation Ltd., Qingdao 266111, China

Corresponding author: Yiqi Zhou (yqzhou@sdu.edu.cn)

This work was supported by the National Key Technology Research and Development Program of China under Grant 2015BAF07B04.

ABSTRACT A resistant muffler is the most direct and effective means of reducing exhaust noise from earthmoving equipment. Different types of construction machinery require different mufflers. Current muffler design is mostly experience-based, and there are blind spots in the design process. The optimization scheme must constantly be revised to achieve satisfactory noise reduction. The use of a large number of optimization schemes are wasteful in terms of both cost and time. Therefore, an effective and time-saving design method for muffler optimization is needed. An optimization approach, known as the “local structural optimization method for a resistant muffler”, based on orthogonal analysis is proposed in this study to optimize the design of a resistant muffler with a complex structure. The results of an orthogonal analysis for a simulation of the muffler structure show that the muffler acoustic and aerodynamic performances are affected by the inlet pipe, outlet pipe, insertion pipe, cross-flow perforated pipe and other local structures, and the results are employed to determine the influence law for the transmission loss (TL) and the exhaust back pressure, considering the local structural parameters of the muffler. The method is applied to optimize the design of a muffler suitable for an excavator and verified by performing an installation test. The experimental results show that the improved designs reduces the exhaust noise by 5 dB and the exhaust back pressure by 0.6 kPa. The improved designs exhibit higher aerodynamic and acoustic performances than a muffler prototype, showing that the proposed method is accurate, effective and reliable. The proposed method considerably simplifies the design process and saves time and cost. This method provides theoretical guidance and an optimization process for the design of a muffler for construction machinery.

INDEX TERMS Resistant muffler with complex structure, orthogonal test, simulation analysis, optimization design.

I. INTRODUCTION

Exhaust noise is one of the main sources of noise from various working machines for which the internal combustion engine is the driving force. An exhaust muffler is the most direct and effective means of reducing exhaust noise from an internal combustion engine; thus, an optimal muffler design has important application value and practical significance [1]. The resistant muffler is the main type of exhaust muffler used in machinery for moving earth. The resistant muffler has a complex structure that consists of a combination of several of muffler units, where the performance of each muffler unit

depends on the muffler structural parameters [2]. The peak exhaust noise frequency band and the transmission loss can be improved by adjusting the local muffler structural parameters to achieve the desired noise reduction performance [3], [4]. Developments in computer simulation technology have made numerical simulation combined with actual vehicle test verification a powerful means for improving muffler performance [5].

The design of a resistant muffler with a complex structure requires the calculation of the aerodynamic and acoustic performances of the muffler based on different multiple structural parameters. Current muffler design is mainly based on using the characteristics of muffler units in conjunction with engineering experience, which inevitably leads to problems, such as unreliable design modifications and a low

The associate editor coordinating the review of this manuscript and approving it for publication was Yue Zhang¹.

optimization efficiency. It is also difficult to achieve optimization goals with few optimization schemes.

Time and cost savings, as well as high efficiency, can be realized by sequencing the influence degree of the structural parameters on the muffler performance to establish an analysis model for local structural optimization and using orthogonal experimental design to optimize the design of the muffler structure [6].

The orthogonal test is a mathematical statistical method in which orthogonal tables are used to analyze multi-factor problems [7]. The number of tests required to obtain the optimal design can be reduced by selecting reasonable test factors and corresponding ranges [8]. An in-depth analysis of the test results can provide the influence rule of each factor on the evaluation indexes.

The orthogonal test has been used to analyze muffler units, such as perforated pipes [9]–[11], and the acoustic performance of mufflers [12], [13] have been optimized with good results. However, those works only optimize the design of a certain muffler unit [14], [5], or only consider acoustics performances without considering aerodynamic performances. An in-depth study has not been performed to determine the law by which structural parameters affect the characteristics of both the acoustics and flow fields of resistant mufflers with complex structures.

Orthogonal analysis theory is used in this study to formulate an optimization design method for a resistant muffler with a complex structure. The effects of structural parameters on the muffler performance are determined by analyzing the simulation results of the orthogonal test scheme, and the optimization method for the local structure is used to solve the optimization efficiency problem and provide a reference for an improved muffler design for engineering applications.

The remainder of the paper is structured as follows. In Section II, the fundamentals of muffler design are presented, and related studies on muffler optimization design are briefly reviewed. In Section III, the procedure for the orthogonal test is presented, and the test results are analyzed in detail. These results are used to propose two improvement schemes in Section IV, and the procedure and results of experiments carried out to compare the actual noise reduction performance of the improved and original schemes are presented. Finally, the conclusions of this study are presented in Section V.

II. FUNDAMENTALS OF MUFFLER AND RELATED WORKS

The structural parameters of the muffler units and a detailed description of a matched muffler suitable for an excavator are presented in this section. Related studies on the application of orthogonal test design to muffler optimization are reviewed in time-series.

A. STRUCTURAL PARAMETERS OF THE MUFFLER UNITS

Exhaust mufflers with complex structures take various forms, where different muffler units are combined to meet specific engineering requirements. The structural parameters of the muffler units significantly impact the performance of

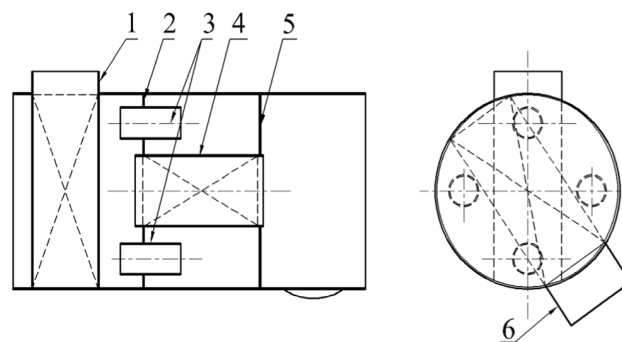


FIGURE 1. Schematic of muffler.

a muffler with a complex structure [15]. The basic design parameters include the overall volume, diameter and length of the muffler [16]; the number of cavities in the muffler; the length and connection mode of each cavity; the diameter and length of the inlet and tail pipes; etc. The muffler performance is affected by specific local structural parameters, such as the perforation rate and diameter of the inlet and outlet pipes; the insertion length and diameter of the inner tube; the aperture and perforation rate of the perforated pipe; and the length of the first cavity [17]. The orthogonal test is a fast and effective way of determining the significance of the structural parameters impacting the muffler performance.

B. MUFFLER WITH A COMPLEX STRUCTURE

A muffler with a complex structure consisting of several classical muffler units is designed with a suitable size for a specific excavator, and an orthogonal simulation is carried out for several structural factors.

The muffler typically has a three-chamber structure. The inlet and outlet pipes are perforated, a cross-flow perforated pipe connects the first and third chambers, and four orthogonally distributed inner pipes connect the first and second chambers. Fig. 1 is a diagram of the structure of the exhaust muffler suitable for the excavator. The following labels are used in the diagram: 1 for the inlet pipe, 2 for the first baffle, 3 for the inner pipes, 4 for the perforated connecting pipe, 5 for the second baffle and 6 for the outlet pipe. Baffles 2 and 5 separate the muffler into three chambers. The diameters of the perforated inlet, connected and outlet pipes are 90 mm, 90 mm and 96 mm, respectively.

C. RELATED WORKS

Orthogonal design is the most widely used method in experimental design and has been applied for more than 70 years. Orthogonal design has been applied to muffler design over the last ten years [9]. Many studies on muffler optimization design have been performed.

Orthogonal experimental design was initially used in conjunction with test experiments [10]. The results of early studies showed that the structural parameters of muffler units, such as the expansion and resonance cavities, significantly impacted acoustic performance [10]. The use of orthogonal

analysis became widespread with the development of three-dimensional numerical simulations. Orthogonal design was combined with finite element analysis to determine the influence degree of different structural parameters on the muffler acoustic performance and obtain optimal structural parameters [11]. GT-Power software was used to test and verify the key structural parameters to evaluate the sum of the muffler transmission loss in the 510 Hz to 640 Hz frequency range [12]. Traditional muffler design theory was incorporated into the design optimization process based on GT-Power [13], [14].

The aforementioned studies generally focus on optimizing a specific muffler unit [5] or evaluating the acoustic performance without considering the aerodynamic performance, and the key structural parameters are not determined on a comprehensive basis.

III. ORTHOGONAL TEST

The optimization method is formulated in this section, and the complete procedure for the orthogonal test is presented. The orthogonal test results are comprehensively analyzed to verify the application of the optimization method.

A. RESEARCH METHODOLOGY

Orthogonal experimental design is a multifactor and multilevel design method [7], [8]. The orthogonal test is used to obtain design schemes by selecting reasonable structural parameters and corresponding ranges. A numerical simulation analysis is used to calculate and analyze the orthogonal test designs to improve efficiency [18].

The following reference indexes are used to evaluate the orthogonal test results in this study: the low-frequency-range (1-500 Hz) noise reduction, the full-frequency-range (1-3000 Hz) noise reduction [19] and the exhaust back pressure. The influence of the structural parameters on the muffler performance is studied. An optimization method for the local muffler structure is presented.

The procedure is as follows. First, the structural design factors for the components of a muffler with a complex structure are extracted, and an orthogonal test is carried out on these factors. Second, a numerical analysis is used to determine the characteristics of the sound and flow fields corresponding to the orthogonal test designs [20], [21]; Third, the orthogonal test results are used to determine the structural factors that significantly affect the sound and flow fields of the muffler, and an optimal design method for the local structure for the muffler based on orthogonal analysis is proposed. Finally, the proposed method is verified by performing an installation test on mufflers designed using the optimized method.

B. ORTHOGONAL TEST DESIGN

The muffler suitable for the excavator mainly consists of perforated pipes, insertion pipes, resonance cavities. The perforated pipe strongly affects the attenuation performance of

the resonator [22]. Limited by finite volume for the engine nacelle and maintaining constant external muffler dimension requires little or no change in the length of the chambers [23], [24]. The perforated and insertion pipes are the main muffler units that affect muffler performances. These two parameters do not interact with each other. The aperture and perforation rate of the perforated pipe significantly affect the muffler performance. According to the influence law of structure parameter sizes on the performance of muffler unit, the value range of structure parameter for the muffler are determined. Table 1 shows the $L_{32}4^9$ orthogonal table [25] used for the orthogonal test analysis. The table shows eight factors without interaction.

Table 2 shows the test schemes determined by the level table for the orthogonal test factors. Table 2 contains 32 schemes, and the effect of the structural parameters on the multichamber muffler can be obtained by analyzing the performances of the schemes.

Note that the error is provided in the ninth column, and random adjustment of the test sequence is not required because there is no randomness in the simulation test.

C. RESULTS OF ORTHOGONAL EXPERIMENT

1) EVALUATION INDEXES

The transmission loss (TL) reflects the level of sound attenuation after exhaust noise passes through silencing elements and is defined as the difference between the incident and transmitted sound power levels. The exhaust back pressure directly affects the engine power loss. The TL over target frequency bands and the exhaust back pressure are the evaluation indexes used in this study.

A 3D software program is used to model the muffler suitable for the excavator. The 3D model is meshed using Hypermesh. Then, the schemes presented in Table 2 are analyzed using the finite element method (FEM) [26]. Virtual lab software is calculate the TL curves for the schemes. The finite element method for the flow field is used in conjunction with Fluent software to calculate the pressure loss for the schemes.

The average noise reduction over the low-frequency (1 Hz-500 Hz) and full-frequency (1 Hz-3000 Hz) ranges are calculated to analyze the influence of the structural parameters on the acoustics characteristics of the muffler performance.

2) RESULTS

The TL curve is obtained from the simulation results for the sound field. First, the total sound pressure is obtained, and the sound pressure level is then calculated to calculate the noise reduction for a specific frequency band.

Equation (1) is used to calculate the TL of the schemes as the evaluation index of the acoustic performance:

$$TL = 10 \lg \left(\frac{W_{in}}{W_{out}} \right) = 10 \lg \left(\frac{p_i^2 A_{in}}{p_o^2 A_{out}} \right). \quad (1)$$

TABLE 1. Orthogonal factor level table of resistant muffler.

factor	level1	level2	level3	level4
A: pore size of inlet perforated pipe(mm)	4	5.5	7	9
B: the perforation rate of inlet perforated pipe	8%	11%	15%	18%
C: pore size of cross flow perforated pipe (mm)	4	5.5	7	9
D: the perforation rate of cross flow perforated pipe	8%	11%	15%	18%
E: pore size of outlet perforated pipe (mm)	5	6.5	8	10
F: the perforation rate of outlet perforated pipe	9%	12%	15%	18%
G: the diameter of insertion pipe (mm)	30	35	40	45
H: the length of insertion pipe (mm)	65	75	85	95

TABLE 2. Orthogonal test scheme.

No.	pore size of inlet perforated pipe(mm)	perforation rate of inlet perforated pipe	pore size of cross flow perforated pipe (mm)	perforation rate of cross flow perforated pipe	pore size of outlet perforated pipe (mm)	perforation rate of outlet perforated pipe	diameter of insertion pipe (mm)	the length of insertion pipe (mm)
1	4	8%	4	8%	5	9%	30	65
2	4	11%	5.5	12%	6.5	12%	35	75
3	4	15%	7	15%	8	15%	40	85
4	4	18%	9	18%	10	18%	45	95
5	5.5	8%	4	11%	6.5	15%	40	95
6	5.5	11%	5.5	8%	5	18%	45	85
7	5.5	15%	7	18%	10	9%	30	75
8	5.5	18%	9	15%	8	12%	35	65
9	7	8%	5.5	15%	10	9%	35	85
10	7	11%	4	18%	8	12%	30	95
11	7	15%	9	8%	6.5	15%	45	65
12	7	18%	7	11%	5	18%	40	75
13	9	8%	5.5	18%	8	15%	45	75
14	9	11%	4	15%	10	18%	40	65
15	9	15%	9	11%	5	9%	35	95
16	9	18%	7	8%	6.5	12%	30	85
17	4	8%	9	8%	10	12%	40	75
18	4	11%	7	11%	8	9%	45	65
19	4	15%	5.5	15%	6.5	18%	30	95
20	4	18%	4	18%	5	15%	35	85
21	5.5	8%	9	11%	8	18%	30	85
22	5.5	11%	7	8%	10	15%	35	95
23	5.5	15%	5.5	18%	5	12%	40	65
24	5.5	18%	4	15%	6.5	9%	45	75
25	7	8%	7	15%	5	12%	45	95
26	7	11%	9	18%	6.5	9%	40	85
27	7	15%	4	8%	8	18%	35	75
28	7	18%	5.5	11%	10	15%	30	65
29	9	8%	7	18%	6.5	18%	35	65
30	9	11%	9	15%	5	15%	30	75
31	9	15%	4	11%	10	12%	45	85
32	9	18%	5.5	8%	8	9%	40	95

where W_{in} and W_{out} are the inlet and outlet sound power levels, respectively; p_i and p_o are the incident and outlet sound

pressures, respectively; A_{in} and A_{out} are the section areas of the muffler inlet and outlet, respectively.

TABLE 3. Orthogonal test results.

NO.	Exhaust back pressure(Pa)	low-frequency noise reduction (dB)	full-frequency noise reduction (dB)
1	16900	1.02	10.97
2	10256	0.90	12.93
3	6650	0.88	13.10
4	5638	0.85	12.86
5	12943	1.20	12.65
6	8521	0.89	12.85
7	9327	1.07	11.51
8	6901	0.84	13.18
9	12015	1.36	12.01
10	7230	0.89	11.32
11	6903	0.98	13.27
12	5610	0.65	12.96
13	8910	2.50	12.45
14	6250	1.45	12.39
15	11290	0.79	12.55
16	7498	1.23	11.09
17	12512	0.79	11.79
18	10205	0.82	12.11
19	7475	1.09	11.91
20	4603	0.89	13.44
21	11826	1.36	12.32
22	8462	0.86	12.54
23	9290	1.04	12.65
24	11093	0.77	12.13
25	11403	1.48	12.18
26	11850	0.74	12.29
27	5507	1.03	13.59
28	5347	0.68	12.20
29	9960	2.50	12.67
30	8010	1.58	11.24
31	6627	0.64	12.33
32	8415	1.03	12.19

The numerically calculated sound field can be used to obtain p_o . Equation (2) can be used to calculate p_i :

$$p_i = \frac{1}{2} (p_1 + \rho c) \tag{2}$$

where p_i is the inlet sound pressure, which is also determined from the numerically calculated sound field, ρ is the air density, and c is the acoustic velocity.

The average noise reduction for a specific frequency band can then be obtained referring to (3):

$$\bar{L}_N = 10 \lg \left[\frac{1}{N} \sum_{f=1}^N 10^{\frac{TL_f}{10}} \right]. \tag{3}$$

Note that the average noise reduction for the low-frequency and the full-frequency ranges is obtained for N of 500 and 3000, respectively.

The flow field pressure at the inlet and outlet nodes is obtained from the flow field simulation. The exhaust back pressure can be expressed as follows:

$$\Delta P = \bar{P}_{in} - \bar{P}_{out}. \tag{4}$$

where \bar{P}_{in} is the average pressure at the inlet, which can be obtained from (5); and \bar{P}_{out} is the average pressure at the

outlet:

$$\bar{P}_{in} = \sum_j^m P_j / m. \tag{5}$$

where P_j is pressure value of a certain node; m is the number of nodes in the inlet section. \bar{P}_{out} can be obtained similarly.

The performance indexes obtained from the simulation results are shown in Table 3. Equation (3) is used to calculate the noise reduction results, and Equation (4) is used to calculate the exhaust back pressure.

Table 4 shows the significance level F obtained from the orthogonal test results. The table shows that $F_{0.01}$ is 29.5 and $F_{0.05}$ is 9.28 [25]. The factors with F above 29.5 strongly significantly affect the test indexes; the factors for which F is between 9.28 and 29.5 significantly affect the test indexes; and the other factors have no significant influence on the test indexes.

D. ANALYSIS OF ORTHOGONAL TEST RESULTS

The influence degree of the structural parameters on the muffler performance can be determined from the significance

TABLE 4. Orthogonal test significance level table of resistant muffler.

factor	F value of back pressure	significance level	F value of low-frequency noise reduction	significance level	F value of full-frequency noise reduction	significance level
A	9.395	*	17.493	*	5.672	
B	78.639	**	25.56	*	4.317	
C	1.568		4.871		1.326	
D	2.986		9.826	*	2.026	
E	11.655	*	3.569		1.892	
F	51.372	**	5.413		9.313	*
G	2.632		0.998		32.240	*
H	0.936		3.469		0.539	

level table. The primary structural parameters that affect the exhaust back pressure are the perforation rate of the inlet and outlet perforated pipes, followed by the pore size of these pipes. Therefore, the inlet and outlet perforated pipes are the key structural parameters that affect the flow-field performance of the muffler. The primary structural parameters for low-frequency noise reduction are the perforation rate and pore size of the inlet perforated pipe, and the perforation rate of the cross-flow perforated pipe. The primary structural parameters that affect the full-frequency-range noise reduction are the diameter of the insertion pipe and the perforation rate of the outlet perforated pipe.

Table 5 presents the results of the orthogonal design direct analysis. The ranges R are calculated from the average values shown for the factors at the \bar{K}_n level to quantitatively evaluate the influence of each factor. The influence of each factor can be quantitatively evaluated from the values of R.

A detailed analysis of the effect of the structural factors is given below.

Factor A: as the pore size of the inlet perforated pipe increases, the exhaust back pressure decreases; increasing the pore size widens the target frequency band and increases the noise reduction, which can be used to adjust the noise-reduction performance of the target frequency band but has a limited contribution to overall noise reduction.

Factor B: the larger the perforation rate of the inlet perforated pipe is, the smaller the exhaust back pressure is, and the smaller the noise reduction for the low-frequency band is. A reasonable perforation rate for the inlet pipe must be selected when considering both the flow-field and low-frequency acoustic performance.

Fig. 2 is a comparison of the TL curves for perforation rates of 11% and 15%. The TL curve for the lower perforation rate corresponds to higher noise reduction over the low-frequency range. The TL in the 500 Hz-1800 Hz range can be increased by increasing the perforation rate. For the frequency band above 1800 Hz, the number of peaks of the curve for the 15% perforation rate increase significantly, and the number of troughs decrease. Different perforation rates correspond to different resonance frequencies. Appropriate perforation rates can be selected to adjust the characteristics of the noise-elimination frequency, thereby achieving the desired noise reduction.

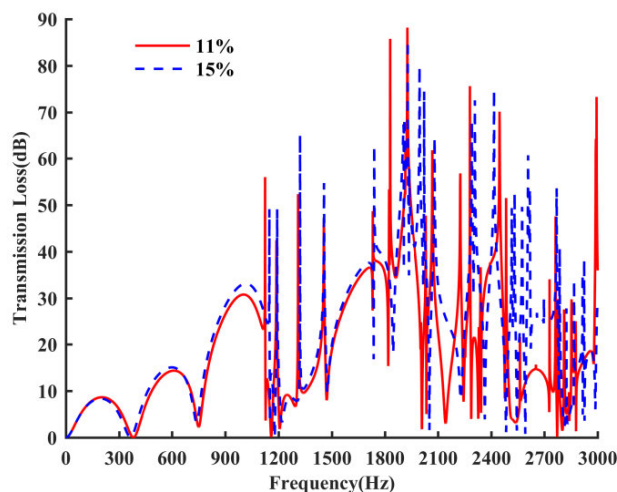


FIGURE 2. Comparison of TL curve with 11% and 15% perforation rate of inlet perforated pipe.

Factor D: the perforation rate of the cross-flow perforated pipe mainly affects the low-frequency noise reduction of the muffler. The low-frequency noise reduction increases with the perforation rate. The perforation rate also affects the exhaust back pressure. The exhaust back pressure decreases as the perforation rate increases.

Factor E: the pore size of the outlet perforated pipe mainly affects the exhaust back pressure. As the pore size increases, the exhaust back pressure first decreases and then remains flat. The lowest exhaust back pressure is obtained at an 8-mm pore size.

Factor F: as the perforation rate of the outlet perforated pipe increases, the exhaust back pressure decreases, the full-frequency-range noise reduction increases, and the low-frequency-range noise reduction does not change significantly. Fig. 3 is a comparison of the TL for 9% and 18% perforation rates of the outlet perforated pipe.

The peak of each TL curve shifts to a higher frequency as the perforation rate increases. Changing the perforation rate has little effect on the noise reduction over the low- and middle-frequency ranges from 0-1200Hz. There is a large TL at the higher perforation rate for the 1900-Hz frequency band. The TL is relatively low at the lower perforation rate over the 2500 Hz to 3000 Hz range and is almost 0 dB at some frequencies. By comparison, the TL can reach 30 dB at the

TABLE 5. Results of orthogonal design-direct analysis.

Index	Factor	Value							
		A	B	C	D	E	F	G	H
exhaust back pressure(Pa)	\bar{K}_1	9321	12074	8979	9336	9455	11322	9245	9011
	\bar{K}_2	9803	8877	8744	9291	9780	9019	8568	8944
	\bar{K}_3	8159	7876	8646	8694	8307	7809	9224	8622
	\bar{K}_4	8439	6895	9352	8401	8180	7571	8684	9145
	R	1645	5179	706	935	1601	3751	676	523
low-frequency noise reduction(dB)	\bar{K}_1	0.9	1.52	0.98	0.97	1.04	0.95	1.1	1.15
	\bar{K}_2	0.99	1.01	1.17	0.88	1.16	0.97	1.14	1.16
	\bar{K}_3	0.97	0.92	1.18	1.16	1.17	1.19	0.97	0.99
	\bar{K}_4	1.45	0.86	0.98	1.31	0.95	1.2	1.11	1.01
	R	0.56	0.66	0.21	0.43	0.21	0.25	0.17	0.18
full-frequency noise reduction(dB)	\bar{K}_1	12.35	12.12	12.35	12.29	12.36	11.96	11.55	12.41
	\bar{K}_2	12.43	12.19	12.34	12.49	12.35	12.17	12.82	12.3
	\bar{K}_3	12.45	12.57	12.24	12.2	12.5	12.56	12.48	12.41
	\bar{K}_4	12.1	12.47	12.41	12.36	12.14	12.65	12.49	12.23
	R	0.35	0.45	0.18	0.29	0.36	0.7	1.27	0.18

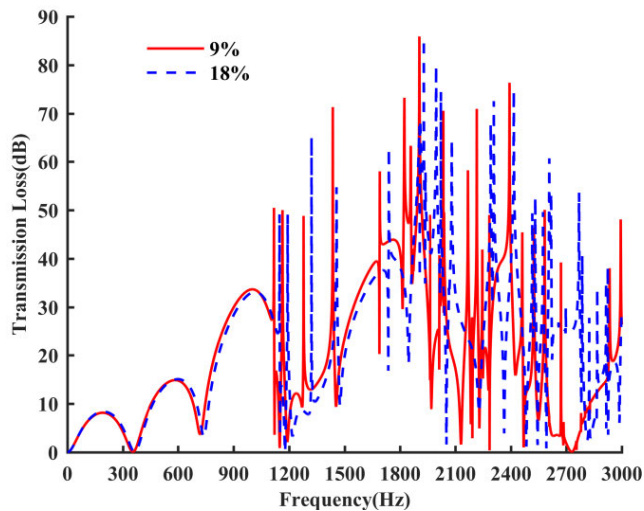


FIGURE 3. Comparison of TL curve with 9% and 18% perforation rate of outlet perforated pipe.

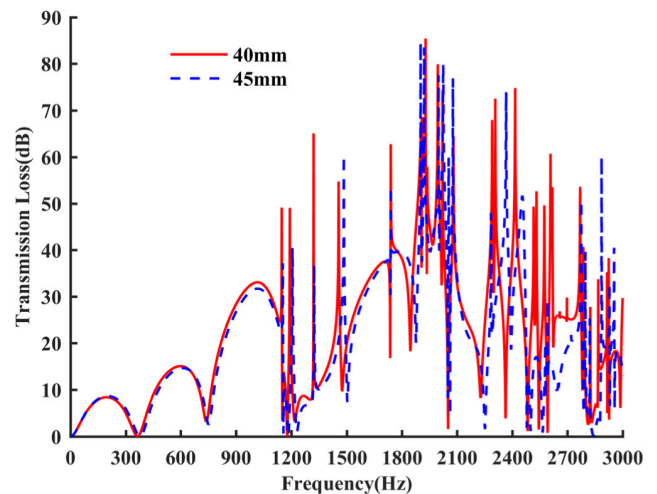


FIGURE 4. Comparison of TL curve with 40mm and 45mm diameter of insertion pipe.

high perforation rate. The TL at the high perforation rate is generally most prominent in the high-frequency band.

Factor G: the insertion pipe diameter mainly affects the full-frequency-range noise reduction. The highest full-frequency-range noise reduction occurs for a pipe diameter of 40 mm. Fig. 4 is a comparison of the TL curves for insertion-pipe diameters of 45 mm and 40 mm. The high degree of coincidence of the two TL curves in the frequency range below 2200 Hz shows that this structural parameter has little effect on noise reduction for low and middle frequencies. However, the TL curve for the 40-mm insertion pipe diameter is clearly dominant for the frequency band centered at 2500Hz. There is no significant difference between the two TL curves for the frequency band at approximately 3000 Hz. The insertion pipe diameter mainly affects the TL of the high-frequency band (at approximately 2500 Hz) and the full-frequency-range noise reduction.

An analysis of the orthogonal test results for the resistant muffler with a complex structure leads to the following conclusions. The results for the aerodynamic evaluation index show that the most important design factors are the perforation rate of the inlet and outlet perforated pipes, followed by the pore size of these pipes. A reasonable perforation rate for the cross-flow perforated pipe should also be selected. The results for the acoustic evaluation index shows that the most important design factors for the low frequency band are the perforation rate and aperture of the inlet perforated pipe, followed by the perforation rate of the cross-flow perforated pipe. The corresponding most important design factors for the full-frequency range are the parameters of the insertion pipe, followed by the perforation rate of the outlet perforated pipe. The perforation rate of the perforated pipes and the insertion pipe parameters affect the peak shifts of specific frequency bands.

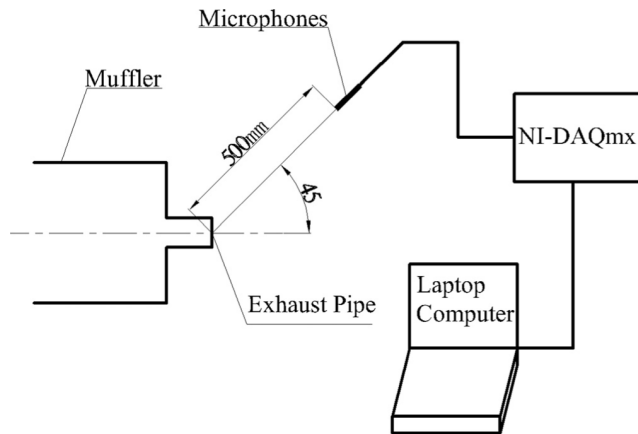


FIGURE 5. Schematic of exhaust noise signal acquisition system.

IV. OPTIMIZATION DESIGN AND EXPERIMENTAL VERIFICATION OF MUFFLERS

The proposed method is used to formulate two optimization schemes in this section. We perform an installation test to verify the effectiveness of the proposed method.

A. OPTIMIZATION SCHEMES

The orthogonal test results are used to guide the optimization design of the original muffler structure, resulting in two improvement schemes.

Scheme 1: The noise reduction performance can be improved considering the flow field characteristics by modifying the muffler structure and optimizing the acoustic performance. The diameter of insertion pipe is set to 40 mm, the perforation rate of cross flow perforated pipe is increased, and the number of holes in the outlet perforated pipe is adjusted appropriately.

Scheme 2: The flow field characteristics can be improved considering the noise reduction performance by modifying the muffler structure and optimizing the flow-field performance. The three-cavity structure is maintained, and the cavity length is changed slightly. The pipe length is reduced, the pore size and perforation rate of the inlet perforated pipe are increased, the perforation rate of the cross-flow perforated pipe is increased, and the number of holes in the outlet perforated pipe is adjusted appropriately.

B. EXPERIMENTAL TEST AND ANALYSIS OF RESULTS

The actual noise reduction performance for the improved schemes is compared against that of the original scheme by installing three mufflers in an excavator and measuring the noise reduction by strictly following the measurement methods and requirements of QC/T631 “Automotive exhaust muffler assembly technical specification and test methods” [27] and GB/T4759-2009 “Exhaust silencers for internal combustion engines - measurement procedure” [28]. Fig. 5 is a schematic of the noise signal acquisition system. The measurement point for exhaust noise is placed at 45° to the axial direction of the exhaust tailpipe and lies 0.5 m from the center point of the end of the exhaust tailpipe and the microphone

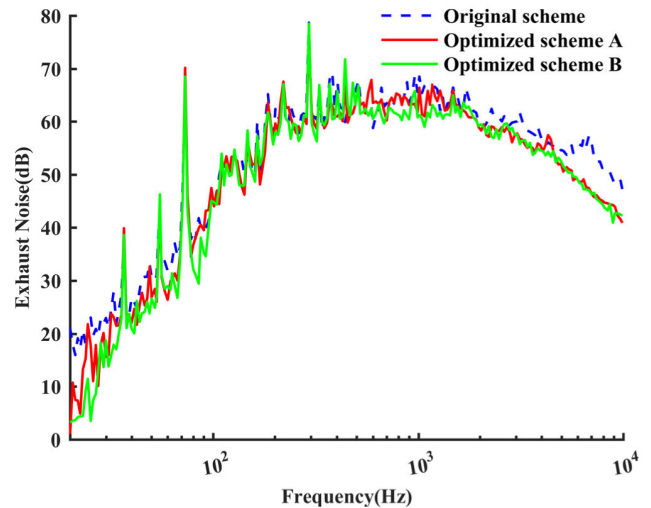


FIGURE 6. Comparison of spectral characteristics of exhaust noise.

location at the exhaust port; the measurement point is more than 1.5 m above ground. The exhaust back pressure of the three mufflers is also measured.

Table 6 shows the exhaust noise measured during the installation test, and Table 7 shows the measured exhaust back pressure of the muffler. The exhaust noise values presented in Table 6 show there is little difference in the total noise reduction by the two improvement schemes during engine idling compared to the original scheme. However, the exhaust noise values of the two improved schemes are significantly lower than that of the original muffler at medium and high engine speeds. The two improved schemes have higher noise reduction at medium and high engine speeds compared to the original muffler. A comparison of the noise for improved schemes 1 and 2 under the same working conditions shows higher noise reduction under scheme 2 than scheme 1. The results presented in Table 7 show that the exhaust back pressure of the improved schemes is lower than that of the original structure, where scheme 2 produces a lower exhaust back pressure than scheme 1.

Fig. 6 shows the spectral characteristics of the muffler exhaust noise to further compare the three muffler performances. The noise amplitude of scheme 2 is reduced by nearly 10 dB compared with the original scheme over the low-frequency band at 20 Hz-30 Hz. There is a peak misalignment at 50 Hz-60 Hz for the noise of scheme 2 compared with that of the prototype, where the amplitude is reduced by nearly 22 dB. A similar result is obtained for scheme 1, for which the corresponding amplitude is reduced by nearly 15 dB. Compared with the original scheme, the noise amplitudes using the two schemes are reduced by at least 6 dB near 1000 Hz and significantly reduced in the high-frequency range above 3000 Hz, where the maximum difference is 10 dB, thereby effectively eliminating the high-frequency noise.

Table 8 shows the sound pressure levels for specific frequency bands at the maximum engine speed for the one-third-octave spectrum of the measured exhaust noises. The optimized schemes exhibit higher acoustic performance than

TABLE 6. Test results of mufflers.

schemes	engine speed (r/min)	background noise (dBA)	exhaust noise (dBA)
original structure	1050	60	75.4
	1800	60	84.4
	2000	60	84.8
	2200	60	85.0
scheme 1	1050	60.3	75.0
	1800	60.3	83.4
	2000	60.3	83.6
	2200	60.3	83.7
scheme 2	1050	62.9	75.5
	1800	62.9	82.7
	2000	62.9	83.1
	2200	62.9	83.3

TABLE 7. Back pressures of mufflers.

schemes	engine speed (r/min)	inlet velocity (m/s)	inlet temperature (K)	inlet pressure (kPa)
original structure	2200	55	483	4.29
scheme 1	2195	55	483	4.01
scheme 2	2200	55	483	3.68

TABLE 8. Sound pressure levels for specific frequency bands.

frequency range (Hz)	1-500	500-1500	1500-3000	1-3000
original structure(dBA)	84.65	82.79	77.74	88.72
scheme 1(dBA)	81.79	79.95	74.42	84.27
scheme 2(dBA)	80.58	77.71	73.58	83.53

the original scheme for all frequency bands. The maximum optimization value is 4 dB over the 1-500Hz frequency band. The maximum optimization value is 5 dB over the 1-3000 Hz frequency band.

Compared with the original structure, the two schemes generally produce the highest noise reduction in the middle and high frequency bands, where the noise reduction of scheme 2 is higher than that of scheme 1 for the middle frequency band. The exhaust back pressure of scheme 2 is smaller than that of the original structure and scheme 1. Therefore, scheme 2 exhibits the highest noise reduction performance and aerodynamic performance.

V. CONCLUSION

A local structural optimization method based on the orthogonal test is presented for a resistant muffler. Experimental results show that the optimized design produces a 5-dB reduction in the exhaust noise and a 0.6-kPa reduction in the exhaust back pressure. The improved proposed scheme exhibits higher aerodynamic and noise-reduction performance than a prototype of the original muffler design. The proposed method solves the problem of reduced optimization efficiency caused by blind spots in the muffler improvement method and serves as a reference for improving muffler design for engineering applications.

The proposed method is summarized. First, the main technical parameters of the internal combustion engine and the performance index of the prototype muffler are used to determine the main structural parameters. Second, an appropriate orthogonal table is selected, the orthogonal test table is populated according to the value range of the main structural

parameters, and then the sound and flow fields of each experimental scheme in the orthogonal table are simulated. Third, the orthogonal test results are analyzed to determine the structural factors that significantly impact the muffler performance, the influence law of the significant structural factors is analyzed, and an optimization scheme based on local structural improvement is proposed for the prototype muffler. Finally, the improved schemes are compared and verified by performing an installation test.

The most important factor for the aerodynamic evaluation index are the perforation rate of the inlet and outlet perforated pipes, followed by the pore size of these pipes. A reasonable perforation rate should also be selected for the cross-flow perforated pipe.

The most important factor for the acoustic evaluation index over the low-frequency band are the perforation rate and aperture of the inlet perforated pipe followed by the perforation rate of the cross-flow perforated pipe. The corresponding most important factors for the full-frequency band are the insertion pipe parameters, followed by the perforation rate of the outlet perforated pipe. The selected perforation rate of the perforated pipes and the insertion pipe parameters can shift the peaks of specific frequency bands.

REFERENCES

- [1] M. L. Munjal, K. N. Rao, and A. D. Sahasrabudhe, "Aeroacoustic analysis of perforated muffler components," *J. Sound Vibrat.*, vol. 114, no. 2, pp. 173-188, Apr. 1987.
- [2] F. D. Denia, A. Selamet, F. J. Fuenmayor, and R. Kirby, "Acoustic attenuation performance of perforated dissipative mufflers with empty inlet/outlet extensions," *J. Sound Vibrat.*, vol. 302, nos. 4-5, pp. 1000-1017, May 2007.
- [3] X. Shi and C.-M. Mak, "Sound attenuation of a periodic array of micro-perforated tube mufflers," *Appl. Acoust.*, vol. 115, pp. 15-22, Jan. 2017.
- [4] J. W. Lee, "Optimal topology of reactive muffler achieving target transmission loss values: Design and experiment," *Appl. Acoust.*, vol. 88, pp. 104-113, Feb. 2015.
- [5] Y. Zhang, P. Wu, Y. Ma, H. Su, and J. Xue, "Analysis on acoustic performance and flow field in the split-stream rushing muffler unit," *J. Sound Vibrat.*, vol. 430, pp. 185-195, Sep. 2018.

- [6] X. M. Xu, H. Jia, Y. P. Zhu, and J. Shi, "Optimization design of muffler based on the theory of orthogonal test," *Appl. Mech. Mater.*, vols. 556–562, pp. 1191–1195, May 2014.
- [7] Z. Xing and W. Guo, "Analysis and research on working performance of shearer based on discrete element method," *IEEE Access*, vol. 7, pp. 121321–121331, Sep. 2019.
- [8] W.-Q. Zhang, X. Sui, B. Yu, Y.-Q. Shen, and H.-L. Cong, "Preparation of high specific surface area and high adsorptive activated carbon by KOH activation," *Integr. Ferroelectr.*, vol. 199, no. 1, pp. 22–29, Jul. 2019.
- [9] J. Fu, M. Xu, Z. Zhang, W. Kang, and Y. He, "Muffler structure improvement based on acoustic finite element analysis," *J. Low Freq. Noise, Vibrat. Act. Control*, vol. 38, no. 2, pp. 415–426, Jan. 2019.
- [10] C. Shen and L. Hou, "Comparison of various algorithms for improving acoustic attenuation performance and flow characteristic of reactive mufflers," *Appl. Acoust.*, vol. 116, pp. 291–296, Jan. 2017.
- [11] A. W. Wankhade and D. A. P. Bhattu, "Optimization and experimental validation of elliptical reactive muffler with central inlet central outlet," *Int. J. Eng. Res.*, vol. 4, no. 5, pp. 1321–1328, May 2015.
- [12] K.-J. Cha, C.-U. Chin, J.-S. Ryu, and J.-E. Oh, "The optimal design for low noise intake system using kriging method with robust design," *JSME Int. J. Ser. C*, vol. 47, no. 3, pp. 873–881, 2004.
- [13] Z. Liu, R. Bi, H. T. Mai, Y. M. Lu, and Y. Wang, "Acoustic characteristic of pass-through and cross-flow dissipative muffler," *Trans. CSICE*, vol. 30, no. 6, pp. 550–556, Nov. 2012.
- [14] F. Xue and B. Sun, "Experimental study on the comprehensive performance of the application of U-shaped corrugated pipes into reactive mufflers," *Appl. Acoust.*, vol. 141, pp. 362–370, Dec. 2018.
- [15] J. Fang, Y. Zhou, X. Hu, and Z. Ling, "CFD simulation of exhaust muffler with complicated structures for an excavator," *Trans. CSICE*, vol. 27, no. 1, pp. 68–73, Jan. 2009.
- [16] S. Ramamoorthy and S. Krishnan, "Towards thermal-acoustic co-design of noise-reducing heat sinks," *IEEE Trans. Compon., Packag., Manuf. Technol.*, vol. 8, no. 8, pp. 1411–1419, Aug. 2018.
- [17] S. Xiao, F. Yan, Z. Liu, and C. Lu, "Study on the acoustic performance of expansion muffler based on comprehensive analysis of acoustic modal and transmission loss," in *Proc. Int. Conf. Inf. Syst. Comput. Aided Educ. (ICISCAE)*, Changchun, China, Jul. 2018, pp. 101–107.
- [18] E. Liu, S. Yan, S. Peng, L. Huang, and Y. Jiang, "Noise silencing technology for manifold flow noise based on ANSYS fluent," *J. Natural Gas Sci. Eng.*, vol. 29, pp. 322–328, Feb. 2016.
- [19] V. Sagar and M. L. Munjal, "Design and analysis of a novel muffler for wide-band transmission loss, low back pressure and reduced flow-induced noise," *Noise Control Eng. J.*, vol. 64, no. 2, pp. 208–216, Mar. 2016.
- [20] H. Zhao and Z. Deng, "Fluid distribution characteristics of occurring flow regeneration noise from muffler element," *Trans. CSICE*, vol. 29, no. 4, pp. 378–383, Jul. 2011.
- [21] W. Zheng, Z. Lin, S. He, and R. Tang, "Study on the adaptive noise control of the ventilation pipeline based on the micro-perforated plate," in *Proc. Int. Conf. Comput. Technol., Electron. Commun. (ICCTEC)*, Dalian, China, Dec. 2017, pp. 1132–1135.
- [22] L. Xiang, S. Zuo, X. Wu, J. Zhang, and J. Liu, "Acoustic behaviour analysis and optimal design of a multi-chamber reactive muffler," *Proc. Inst. Mech. Eng., D, J. Automobile Eng.*, vol. 230, no. 13, pp. 1862–1870, Nov. 2016.
- [23] S. Zuo, K. Wei, and X. Wu, "Multi-objective optimization of a multi-chamber perforated muffler using an approximate model and genetic algorithm," *Int. J. Acoust. Vibrat.*, vol. 21, no. 2, pp. 152–163, 2016.
- [24] S. Nag, A. Gupta, and A. Dhar, "Effect of geometric parameters on the acoustical performance of single inlet single outlet expansion chamber muffler," in *Proc. Int. Conf. Electr., Electron., Optim. Techn. (ICEEOT)*, Tamilnadu, India, Mar. 2016, pp. 2522–2526.
- [25] K. Fang and C. Ma, "Orthogonal design of experiment," in *Orthogonal and Uniform Experimental Design*, vol. 1, 1st ed. Beijing, China: Science Press, 2001, pp. 35–77.
- [26] Y. Jie, "Numerical analysis of internal flow field of complex muffler," in *Proc. IEEE 8th Joint Int. Inf. Technol. Artif. Intell. Conf. (ITAIC)*, Chongqing, China, May 2019, pp. 1758–1762.
- [27] *Automotive Exhaust Muffler Assembly Technical Specification and Test Methods*, Standard QC/T 631-2009, 2009.
- [28] *Exhaust Silencers for Internal Combustion Engines-Measurement Procedure*, Standard GB/T 4759-2009, 2009.



RUI LI was born in Dezhou, China, in 1989. He received the B.S. degree from the College of Mechanical and Electronic Engineering, Shandong University of Science and Technology, Qingdao, China, in 2011, and the M.S. degree in mechanical and electronic engineering from Shandong University, in 2015, where he is currently pursuing the Ph.D. degree. His main research interests include acoustics, aerodynamics, and digital signal processing.



YIQI ZHOU received the Ph.D. degree in mechanical engineering from Shandong University, in 2002. He is currently a Professor with the School of Mechanical Engineering, Shandong University, where he is also the Head of the Virtual Engineering Research Center. He is a Senior Member of the Society for Experimental Mechanics (SEM), the robotics and computer integrated manufacturing, the Chinese Institute of Electronics, and the Chinese Mechanical Engineering Society. His current research interests include vibration and noise control, dynamics of mechanical systems, and virtual reality engineering.



YUAN XUE was born in Yantai, China, in 1988. He received the B.S. and M.S. degrees in mechanical engineering from Shandong University, Jinan, China, in 2010 and 2013, respectively. He is currently an Engineer at CRRC Qingdao Sifang Corporation Ltd., Qingdao, China. His research interests include high-speed EMU designing and acoustics.



SU HAN was born in Jinan, China, in 1990. She received the B.S. and M.S. degrees in industrial design from Shandong University, Jinan, China, in 2013 and 2016, respectively, where she is currently pursuing the Ph.D. degree. Her research interests include ontology, knowledge sharing, and digital signal processing.

...